Third International Symposium on Marine Propulsors
smp'13, Launceston, Tasmania, Australia, May 2013

The Modeling of Hub Vortex for Numerical Analysis of Marine Propeller Using a Simple Surface Panel Method "SQCM"

Takashi Kanemaru[1], Tomohiro Ryu[2], Akira Yoshitake[1], Jun Ando[1], Kuniharu Nakatake[3]

[1]Faculty of Engineering, Kyushu University, Japan
[2]Shin Kurushima Dockyard Co., LTD., Japan
[3]Professor Emeritus, Kyushu University, Japan

ABSTRACT

This paper presents a modeling of hub with hub vortex for numerical analysis. We use our original surface panel method "SQCM" and modify previous SQCM to new model with hub vortex. In SQCM, Hess and Smith type source panels are distributed on the propeller blades and hub surface. And discretized vortices are distributed on the camber surfaces according to Lan's QCM. In this method, we regard the hub as the part of blade and extend the end of lifting surface from the root of blade to the center line of propeller. First, the calculation method is described. Next, reasonable calculated results about hub surface flow, hub pressure distribution and hub wake are presented. Moreover, we conduct propeller open test which measures the thrust and torque of blades and boss cap separately in order to measure the boss cap drag. Finally, the comparison between calculated boss cap drag and experimental one is shown and discussions are made.

Keywords

SQCM, Hub Vortex, Root Vortex, Hub Surface Flow, Slip Stream behind Hub

1 INTRODUCTION

Panel methods are widely used for prediction of propeller performance. These can include the hub body effect by panel arrangement on hub surface. However hub vortex is commonly out of consideration because the treatment is difficult in modeling. In the calculation without hub vortex, the blade root is treated as blade tip, so that the root section must shed strong vortex. The calculated hub force is not usually included into propeller performance because it probably contains numerical error. Hub vortex may be not so important if the calculation is about single propeller performance. On the other hand, hub vortex is sometimes very important about such as interaction problem, calculation of propeller with energy saving device, and so on. For this reason, we need more real and practical propeller model considering both hub surface and hub vortex.

We know that blade root has mirror image effect which keeps non-zero circulation and hub vortex is shed from the end of boss cap. According to the phenomenon, hub has to be treated as tip of all blades, and hub vortex has to be shed as tip vortex from the end of boss cap. Regarding lifting surface theory, several studies have been made on hub vortex as shown by Wang (1985). These basic approaches are that the slope of circulation is zero at blade root and there is an image effect in order to satisfy that condition.

In Kyushu University, we developed a simple surface panel method "SQCM" (Source and QCM) and confirmed that SQCM gives accurate solutions for every problem such as unconventional propeller, cavitating propeller. This paper presents a new model of SQCM, which can express hub effect exactly using the numerical characteristic in SQCM. SQCM consists of "QCM" (**Q**uasi-**C**ontinuous vortex lattice **M**ethod) (Lan 1974) and Hess and Smith type source panel method (Hess & Smith 1964). In this method, we modify the treatment around root on the lifting surface according to QCM. We find that our present method shows reasonable results without singularity regarding hub surface flow, hub wake, and so on. As one of methods to validate our new model, we conducted experiment which measured boss cap drag using high speed circulating water channel of Kyushu University. In this paper, we show the calculation method, calculated results and validation using experimental data. We take only steady propeller problem in this paper.

2 CALCULATION METHOD

2.1 Outline of SQCM

SQCM uses source distributions according to Hess and Smith method on the propeller blade including hub surface and discrete vortex distributions arranged on the mean camber surface according to QCM, which is well known as one of lifting surface methods. These singularities should satisfy the boundary condition that the normal velocity is zero on the propeller blade, hub surface and mean camber surfaces. The formulation of SQCM was described in the papers (Ando et al 1998), (Kanemaru and Ando 2009). In this section, we describe

the calculation method for steady problem in order to help understanding our new model.

Consider a K – bladed propeller rotating with a constant angular velocity Ω (= $2\pi n$, n :number of propeller revolutions) in inviscid, irrotational and incompressible fluid. The space coordinate system $O-XYZ$ and the propeller coordinate system $o-xyz$ are introduced as **Figure 1**. The cylindrical coordinate system $o-xr\theta$ is also introduced for convenience. Then the following relation transforms the cylindrical coordinate system $o-xr\theta$ into the propeller coordinate system $o-xyz$.

$$x = x,\ y = -r\sin\theta,\ z = r\cos\theta \tag{1}$$

Where $r = \sqrt{y^2+z^2}$, $\theta = \tan^{-1}(-y/z)$

The propeller blade S_B is divided into M panels in the spanwise direction. The face and back surfaces of the blade section are divided into N panels in the chordwise direction, respectively. Therefore the total number of source panels becomes $(M\times 2N)\times K$ and constant source m is distributed in each panel. The hub surface S_H is also divided into quadrilateral panels. The velocity vector $\vec{V}_m$ due to the source distributions on the blade surfaces and hub surface is expressed by using velocity potential Φ_m as

$$\vec{V}_m = \nabla\Phi_m \tag{2}$$

Where

$$\Phi_m = -\frac{1}{4\pi}\iint_{S_B+S_H}\frac{m(x',y',z',t')}{\sqrt{(x-x')^2+(y-y')^2+(z-z')^2}}dS$$

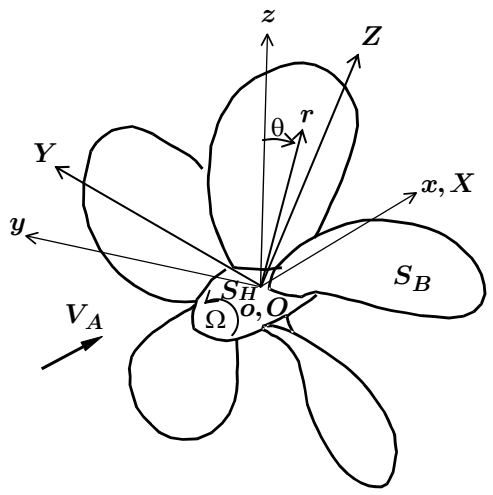

Figure 1 Coordinate systems of propeller

Next the mean camber surface is divided into M segments in the spanwise direction corresponding to the division of the source panels and divided into N_γ in the chordwise direction. Here we introduce ξ axis whose origin locates at the leading edge and is extended to the trailing vortex surface along the mean camber surface. The position of the bound vortex $\xi_{\mu\nu}^{LP}$ and control point $\xi_{\mu\nu}^{CP}$ on the mean camber surface are expressed by the following equations according to the QCM theory.

$$\begin{aligned}\xi_{\mu\nu}^{LP} &= \xi_L(\eta_\mu) + \frac{\xi_T(\eta_\mu)-\xi_L(\eta_\mu)}{2}\left(1-\cos\frac{2\nu-1}{2N_\gamma}\pi\right)\\ \xi_{\mu\nu}^{CP} &= \xi_L(\bar{\eta}_\mu) + \frac{\xi_T(\bar{\eta}_\mu)-\xi_L(\bar{\eta}_\mu)}{2}\left(1-\cos\frac{\nu}{N_\gamma}\pi\right)\end{aligned} \tag{3}$$

Where $\bar{\eta}_\mu = \frac{1}{2}(\eta_\mu+\eta_{\mu+1})$

μ and ν are numbers in the spanwise and chordwise directions. $\xi_L(\eta_\mu)$ and $\xi_T(\eta_\mu)$ are the positions of the leading edge(L.E.) and trailing edge(T.E.), respectively. And total $(M\times N_\gamma)\times K$ horse shoe vortices are located on the mean camber surface according to Equation (3) as illustrated in **Figure 2**. A horse shoe vortex consists of one bound vortex, two free vortices and two streamwise trailing vortices. Here streamwise trailing vortices leave the trailing edge in the direction tangential to the mean camber surfaces and the pitch of trailing vortices reaches an ultimate value, which is the mean of the geometrical pitch distribution of the propeller blade, within a half revolution.

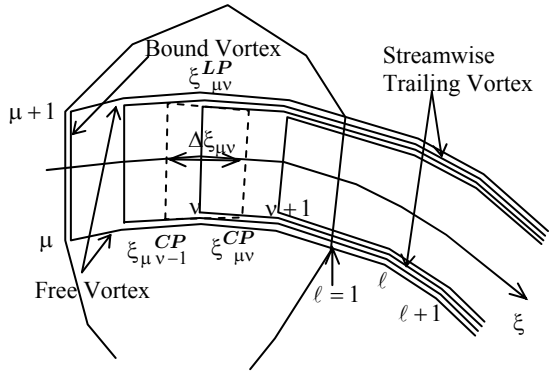

Figure 2 Arrangement of vortex systems

We define the induced velocity vector due to a horseshoe vortex of unit strength as

$$\vec{v}_{k\mu\nu}^{\gamma} = \vec{v}_{k\mu\nu}^{B} + \sum_{\nu'=\nu}^{N_\gamma}\left(\vec{v}_{k\,\mu+1\nu'}^{F} - \vec{v}_{k\mu\nu'}^{F}\right) + \sum_{\ell=1}^{N_w}\left(\vec{v}_{k\,\mu+1\ell}^{T} - \vec{v}_{k\mu\ell}^{T}\right) \tag{4}$$

Where

$\vec{v}_{k\mu\nu}^{B}$ = induced velocity vector due to the bound vortex of unit strength on the mean camber surface

$\vec{v}_{k\mu\nu}^{F}$ = induced velocity vector due to the free vortex of unit strength on the mean camber surface

$\vec{v}_{k\mu\ell}^{T}$ = induced velocity vector due to the streamwise trailing vortex of unit strength on the wake surface

The induced velocity vector due to each line segment of vortex is calculated by the Biot-Savart law.

If we define the strengths of the horseshoe vortex on the mean camber surface, the induced velocity vector due to the vortex model of the QCM theory is given by the following equation.

$$\vec{V}_\gamma = \sum_{k=1}^{K}\sum_{\mu=1}^{M}\sum_{\nu=1}^{N_\gamma}\gamma_{k\mu\nu}\vec{v}^{\gamma}_{k\mu\nu}\Delta\xi_{\mu\nu} \quad (5)$$

Where

$$\Delta\xi_{\mu\nu} = \frac{\pi c(\bar{\eta}_\mu)}{2N_\gamma}\sin\frac{2\nu-1}{2N_\gamma}\pi$$

$c(\bar{\eta}_\mu)$ =chord length of μ section

In this way, the velocity vector $\vec{V}$ around a propeller in the propeller coordinate system is expressed as

$$\vec{V} = \vec{V}_I + \vec{V}_\gamma + \vec{V}_m \quad (6)$$

Where $\vec{V}_I$, $\vec{V}_\gamma$ and $\vec{V}_m$ are inflow, induced velocity vectors due to vortex and source distributions, respectively.

The boundary conditions at the control points on the blade, hub and mean camber surfaces are that there is no flow across the surfaces. Therefore the equation of the boundary condition is given as follow:

$$\vec{V}\cdot\vec{n} = 0 \quad (7)$$

Where $\vec{n}$ is the normal vector on the blade, hub and mean camber surfaces.

The pressure distribution on the propeller blade is calculated by the Bernoulli equation expressed as

$$p - p_0 = -\frac{1}{2}\rho\left(\left|\vec{V}\right|^2 - \left|\vec{V}_I\right|^2\right) \quad (8)$$

Where

p_0 = the static pressure in the undisturbed inflow

ρ = the density of the fluid

The pressure of the propeller blade is expressed as the following pressure coefficient C_{pn} in order to compare the calculated results with experimental data.

$$C_{pn} = \frac{p - p_0}{\frac{1}{2}\rho n^2 D^2} \quad (9)$$

Where D is the diameter of the propeller.

The thrust T and the torque Q of the propeller are calculated by pressure integration. Denoting the $x-$, $y-$ and $z-$components of the normal vector on the blade surface by n_x, n_y and n_z, respectively, the thrust and the torque are expressed by

$$T = \iint_{S_B}(p - p_0)n_x dS$$
$$Q = \iint_{S_B}(p - p_0)(n_y Z - n_z Y)dS \quad (10)$$

Finally the advance coefficient J, the thrust and the torque coefficients K_T, K_Q are expressed as follows:

$$J = \frac{V_A}{nD}, K_T = \frac{T}{\rho n^2 D^4}\ K_Q = \frac{Q}{\rho n^2 D^5} \quad (11)$$

2.2 Hub Vortex Model

The described method at **2.1** includes the hub surface but did not consider hub vortex. Therefore, it is general that the hub surface has to be excluded from pressure integral area for calculation of propeller performance shown by Equation (10). In the present method, we assume that hub is the tip of all blades and hub vortex as tip vortex sheds from the end of boss cap. According to this assumption, we added a row of horse shoe vortex defined by QCM inside the hub (**Figure 3 and 4**). These bound vortex distribution should be determined by a theoretical condition. We distribute same strength vortices to those on the first root section for simplicity. In this case, there are two same strength vortices on the root vortex line and the directions are opposite each other. As the result, the root vortex vanishes. On the other hand, the hub vortex as tip vortex exists on the center line of propeller. This model satisfies the condition that the slope of circulation at root section is zero. In this way, hub vortex sheds from the end of boss cap as tip vortex without singularity. The strength of root vortex may not be perfectly zero with non-zero slope of circulation, but this is our future works. In this method, we adopt Rankine vortex model to express hub vortex in order to avoid too strong negative pressure at the end of boss cap. We should consider the viscous effect to decide the separation point and the radius of vortex core, theoretically. This is our future work, too.

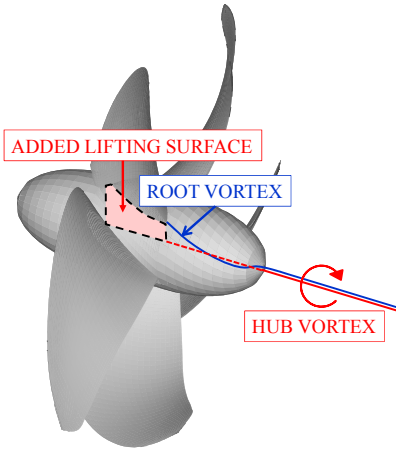

Figure 3 Outline of hub vortex model

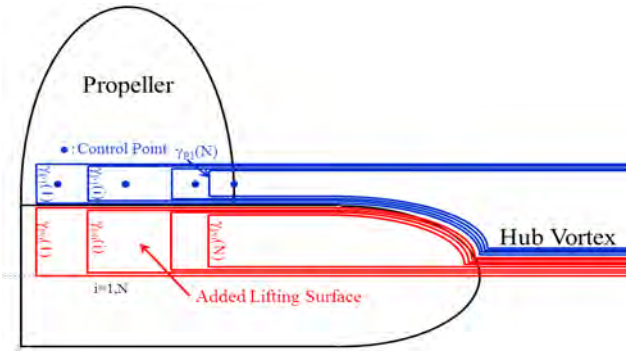

Figure 4 Modeling of lifting surface around root

3 CALCULATED RESULTS

First of all, we take Seiun-Maru-I conventional propeller (CP) for an example of calculation. **Table 1** shows the principal particulars of propeller and **Figure 5** shows the panel arrangement of the propeller. The shape of boss cap is elliptical and the shape in front of blades is cylindrical. The present method is performed with three different radiuses of hub vortex core in order to investigate the effect. Also, we add the calculated results by previous method without hub vortex. In the previous method, there is the hub surface in order to consider the displacement effect of hub as well as new model but not the hub vortex (**Figure 6**).

Table 1 Principal particulars of Seiun-Maru-I CP

DIAMETER (m)	0.22095
PITCH RATIO AT 0.7R	0.95
EXPANDED AREA RATIO	0.65
BOSS RATIO	0.1972
NUMBER OF BLADE	5
SKEW ANGLE (DEG.)	10.5
RAKE ANGLE (DEG.)	6.0
BLADE SECTION	MAU

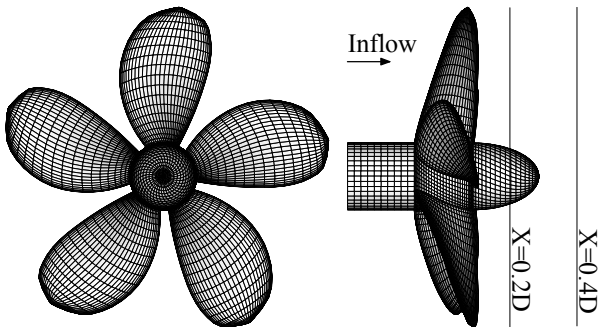

Figure 5 Panel arrangement of Seiun-Maru-I CP

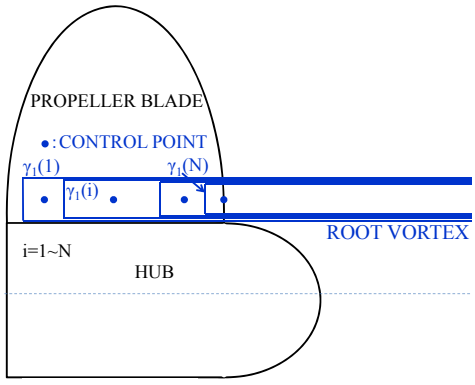

Figure 6 Simplified hub vortex model in previous method

Figure 7 shows the calculated thrust and torque by different radius of hub vortex core comparing with the results by previous method. The core radiuses are 5%, 15% and 25% to the boss cap radius. The thrust by 5% core radius is smaller than other results in heavy loading condition. The cause of this thrust reduction is strong negative pressure at the end of boss cap by the singularity of hub vortex line. On the other hand, the thrust by previous method is larger than those by present method. We have to investigate the core radius considering theoretical viscous effect as our further research though the difference between the results by 15% and 25% is small.

Figure 8 shows the calculated thrust and torque by pressure integral on blade surfaces without hub surface. We can hardly see the differences among these calculated results. This denotes that hub vortex model does not affect blades and only hub force affects propeller performance.

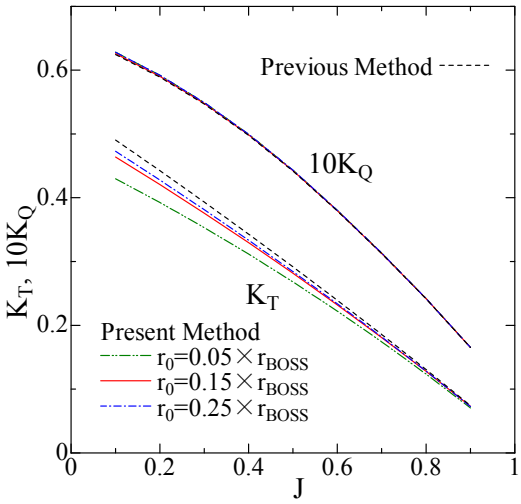

Figure 7 Comparisons of KT and KQ with hub surface

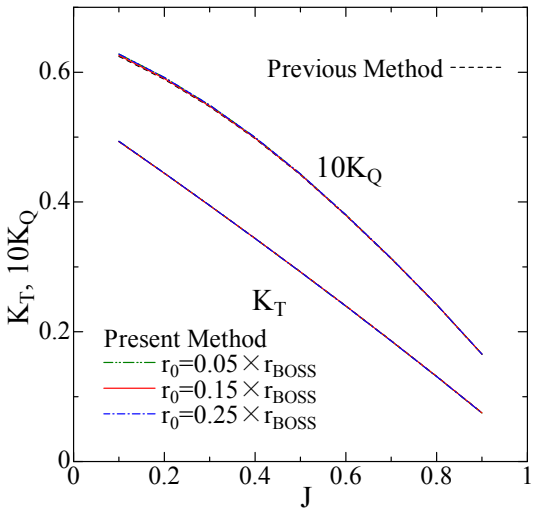

Figure 8 Comparisons of KT and KQ without hub surface

Figure 9 shows the comparison of circulation distribution between present method and previous one. The remarkable point is the difference around blade root. We can see the mirror image effect at blade root which keeps the non-zero circulation. On the other hand, the root circulation by previous method decreases toward zero as well as that of blade tip.

Figure 10 helps understanding this result. The pressure distributions of 0.3R section are almost same between present method and previous method. On the other hand, the results of 0.2R section, namely root section are much different each other. At this section, the pressure distribution by present method shows stable one without tip effect. On the other hand, the result of previous method shows the negative pressure peak near the trailing edge. This is the characteristic of tip section. Even if hub surface panels are arranged, the calculated phenomenon of root section is same to one of tip section.

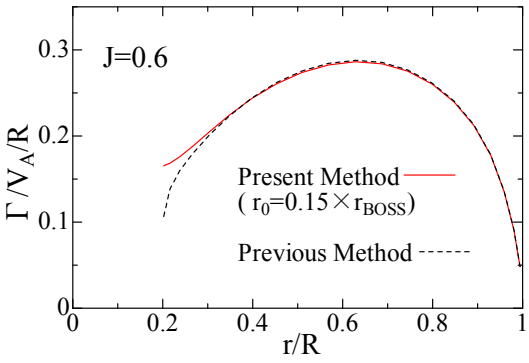

Figure 9 Comparison of circulation distributions

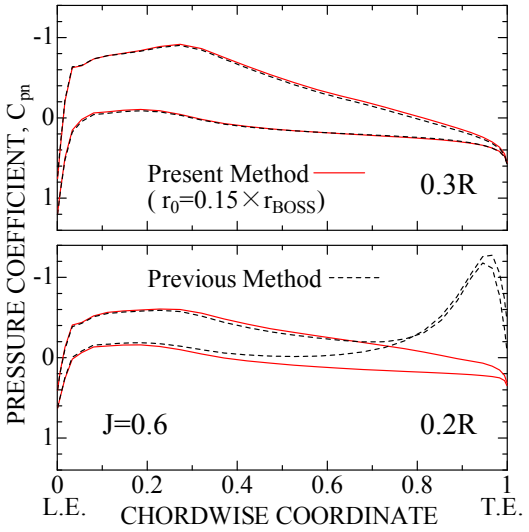

Figure 10 Chordwise pressure distributions

Figure 11 shows the pressure distribution on blades and hub surface. The strong negative pressure by hub vortex at the end of boss cap can be seen in the result of present method. On the other hand, the negative pressure is not so large in previous method. This difference is the reason that the thrust by present method is smaller than that by previous method (see **Figure 7**).

Figure 12 shows the comparison of hub surface flows. It is interesting that the result by present method expresses well the flow with hub vortex. On the other hand, we cannot see the vortex flow around the end of boss cap in the result by previous method. From **Figures 11** and **12**, it seems that our present method gives reasonable solutions.

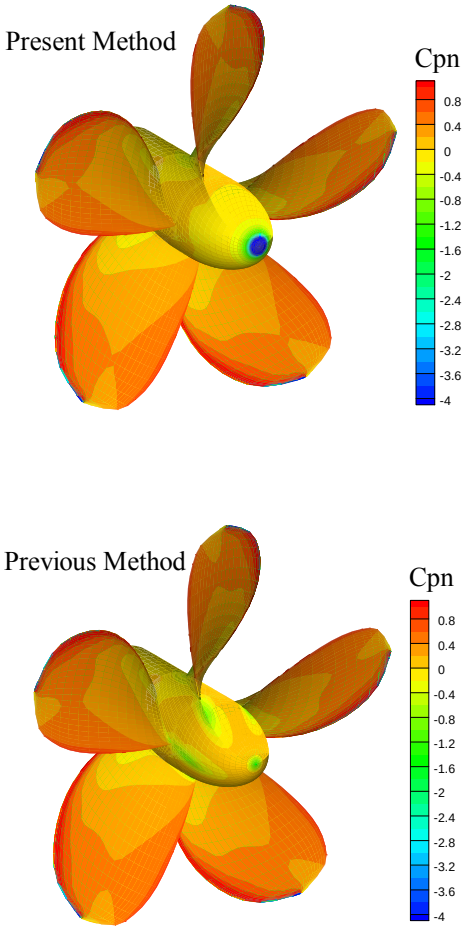

Figure 11 Comparison of pressure distributions

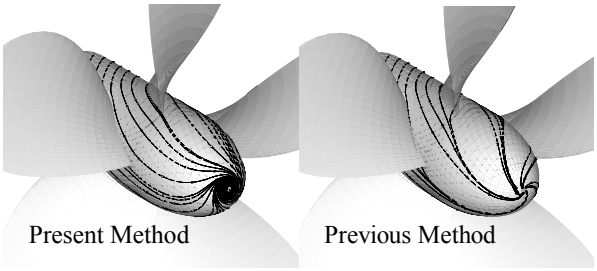

Figure 12 Comparison of streamlines on boss caps

Figures 13 and **14** show the axial and tangential velocities of slip stream. The differences between present method and previous method can be seen behind the hub. The present method accelerates the axial velocity of slip stream including the hub wake. Also, strong tangential velocity around hub vortex is expressed by present method. By the way, the tangential velocity by present method is not infinite on the hub vortex. This is due to Rankine vortex model which treats the flow near the hub vortex line as the solid body.

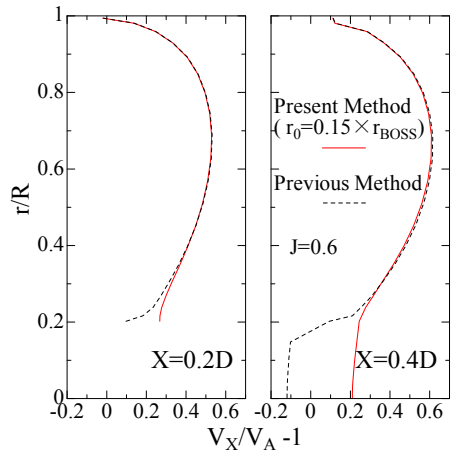

Figure 13 Axial velocities of slip stream

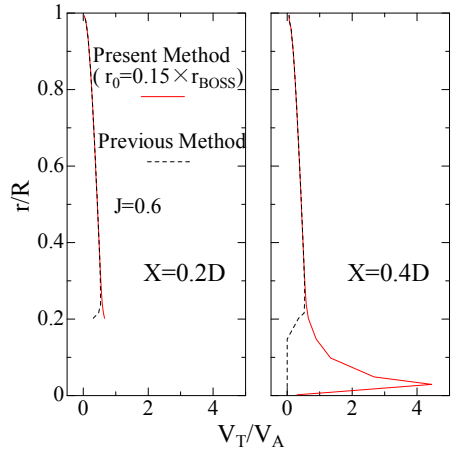

Figure 14 Tangential velocities of slip stream

4 EXPERIMENT

If our new model is valid, we should be able to calculate the boss cap drag, qualitatively. In order to confirm it, we conduct special propeller open test in our facility, which measures the thrust and torque of blades and a boss cap separately. **Figure 15** shows our high speed circulating water channel of Kyushu University. We took two propellers which are Propeller A and Propeller B. **Table 2** shows the principal particulars of these propellers and **Figure 16** shows the photo of propeller A from suction side. They have different pitch distributions each other but other particulars are same. Propeller A is an original propeller of product tanker and Propeller B is optimized propeller from propeller A as the original propeller (Ando et al. 2010).

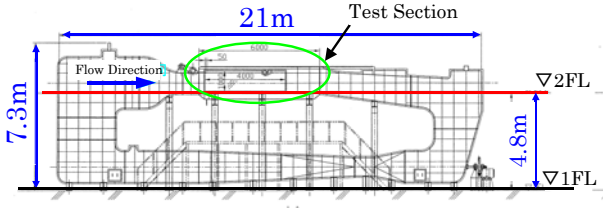

Figure 15 High speed circulating water channel

Table 2 Principal particulars of propellers

	Propeller A	Propeller B
DIAMETER (m)	0.25	0.25
PITCH RATIO AT 0.7R	0.6528	0.6382
OPERATION POINT J	0.4305	0.4305

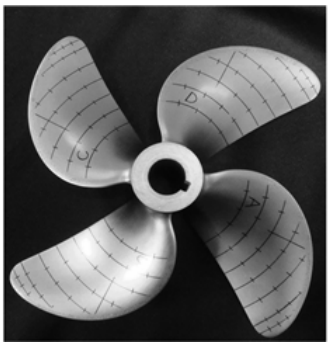

Figure 16 Propeller A

Figure 17 shows the measurement system in order to measure the thrust and torque of propeller blades and a boss cap separately. We used two propeller open boats (POB). The large one measures those of propeller blades in the same manner to opposite propeller open test. And the small one measures those of boss cap from downstream side thorough the boss cap shaft. Propeller and boss cap work at same number of revolution. **Figure 18** shows the state of working propeller and boss cap.

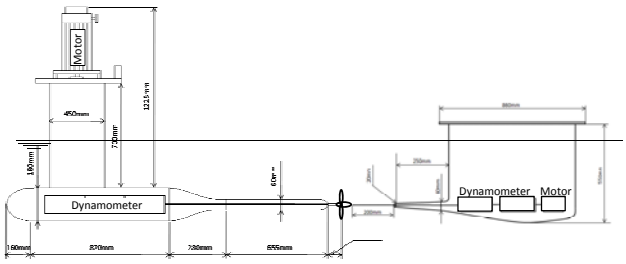

Figure 17 Measurement system for propeller blades and boss cap

There is a small gap between propeller and boss cap to separate these forces as shown in left side of **Figure 19** (Measurement I). However, the measured force by small POB includes the force of boss cap shaft. In order to get rid of this force, we added one more measurement that the gap is between boss cap and boss cap shaft as shown in right side of **Figure 19** (Measurement II). We obtained the boss cap drag by subtracting the force of Measurement II from the one of Measurement I. It is noted that the absolute value of boss cap drag is very small. It is less than 1% of propeller thrust at the design point. Also, it is inevitable that the boss cap shaft interrupts the developing of hub vortex though the radius of shaft is sufficiently small. In any event, it is very difficult to get quantitatively accurate data. However, we are interested in only qualitative difference between these two propellers.

Figure 18 Working propeller and boss cap with same number of revolution

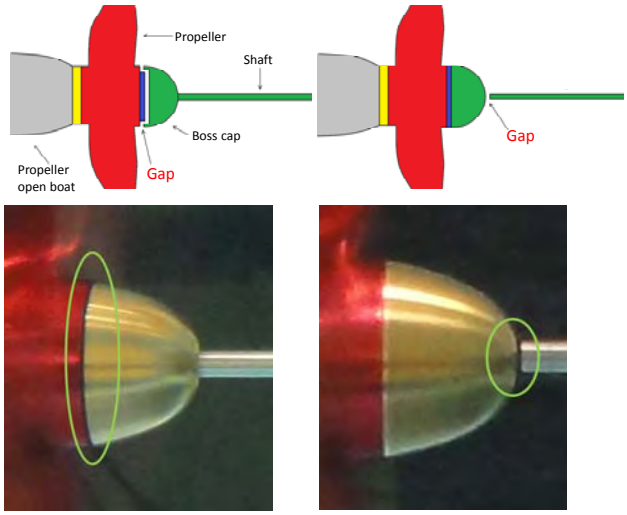

Figure 19 Measurement I (Left) and measurement II (Right)

5 VALIDATION OF BOSS CAP FORCE

Figure 20 shows the panel arrangement for experimental model which has a part of boss cap shaft.

Figure 21 shows the calculated and measured boss cap components of thrust coefficient. In this figure, negative thrust means the boss cap drag. Qualitative agreement can be seen between experimental data and calculated results, in which, the boss cap drag of propeller B is smaller than propeller A. Also, calculated results express the tendency of drag with loading condition. The positive thrust can be seen at low loading condition. This is because stagnated positive pressure affects the end of boss cap in the case that hub vortex is very small. On the other hand, there is no stagnation point because the hub shape is not closed in the front shown in **Figure 20.** Our calculation method is based on potential flow theory and we do not consider viscous effect. Therefore, there are some cases that the force of hub becomes positive thrust in calculation.

Figure 22 shows the comparison of circulation distributions. This figure explains the results of **Figure 21**. The maximum circulation of Propeller B is around 0.7R section. This is tip side comparing with Propeller A. As the result of optimization, the circulation peak shifts to tip side. Instead of that, the circulation of root side which decides the strength of hub vortex becomes small. **Figures 21** and **22** show that present method can predict the qualitative boss cap force resulting from the characteristic of propeller blade.

Figure 23 shows the comparison of pressure distributions. The negative pressure on the boss cap shaft of Propeller B is weaker than that of Propeller A. This is corresponding to **Figure 21**

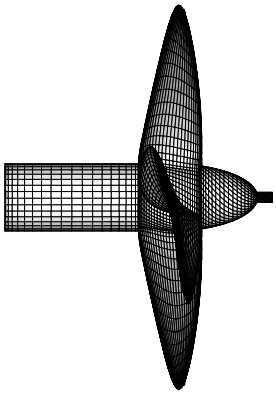

Figure 20 Panel arrangement of experiment model

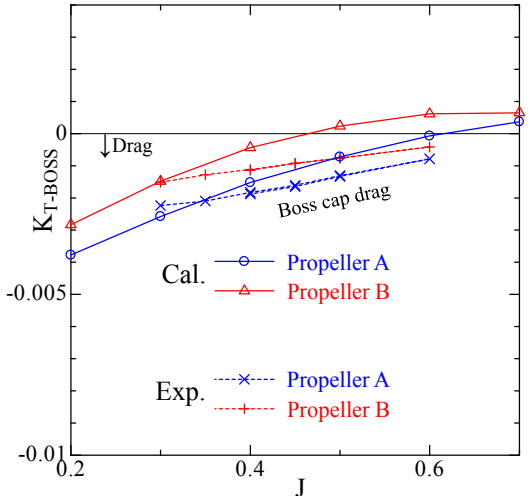

Figure 21 Boss cap components of thrust coefficient

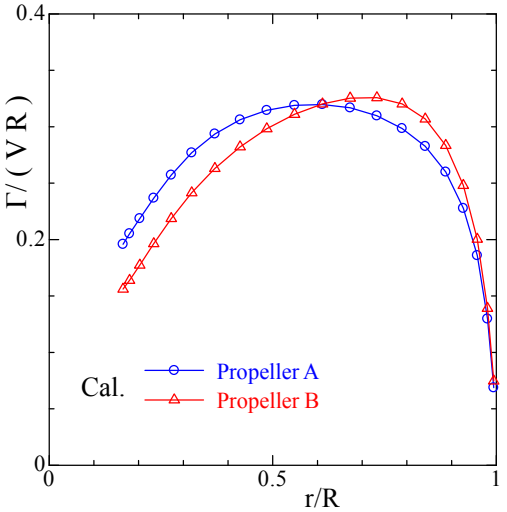

Figure 22 Comparison of circulation distributions

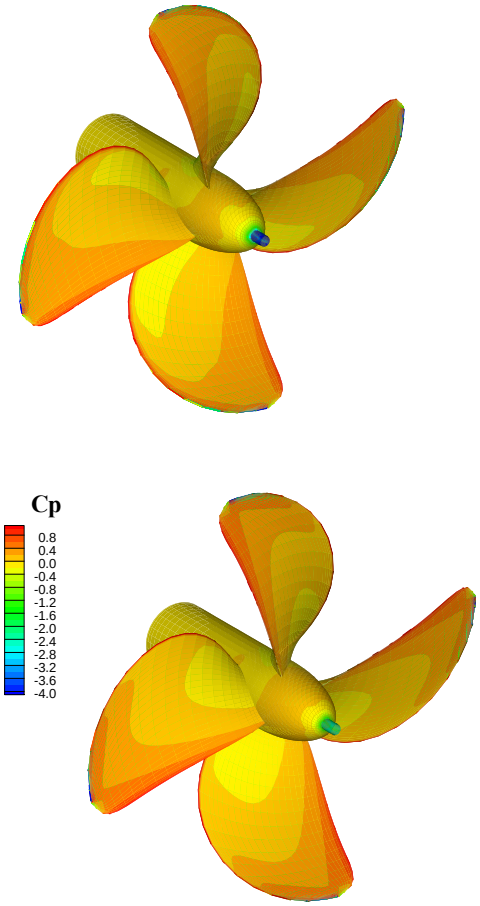

Figure 23 Comparison of pressure distribution (Upper: Propeller A, Lower: Propeller B)

6 CONCLUSION

In this paper, we presented a calculation method that can consider not only hub surface but also hub vortex modifying a simple surface panel method "SQCM". In this method, we consider the hub as the tip of all blades and extend the lifting surface according to QCM to center line of propeller through the hub surface. Also, we conducted the experiment to measure the boss cap drag as comparison data with calculated results. As the results of validation, following conclusions were led.

(1) The calculated propeller performance expresses the thrust reduction by only boss cap drag. The drag depends on the size of hub vortex core, but the difference by core size is very small if it is not so small.

(2) The calculated hub surface flow is reasonable, in which the flow merges at the end of boss cap and becomes hub vortex. As the result, negative pressure can be seen at the end of boss cap.

(3) The circulation of root section keeps the strength to express the mirror image effect. Because of it, the pressure distribution around root section shows reasonable results.

(4) It is confirmed by experimental data that present method can calculate the boss cap drag, qualitatively. The boss cap drag depends on the strength of hub vortex, namely, the circulation at blade root or the loading condition.

We are going to apply present method to various problems which need hub vortex model. However, present method is not enough to predict the hub effect, quantitatively. In our future works, we are going to study how to decide the size of hub vortex core or the strength of root vortex.

REFERENCES

Ando, J., Maita, S. & Nakatake, K. (1998). 'A New Surface Panel Method to Predict Steady and Unsteady Characteristics of Marine Propeller'. Proceedings of 22nd Synposium on Naval Hydrodynamics, Washington D.C., pp. 142-154.

Ando, J., Kataoka, S. & Ryu T. (2010). 'A Method to Improve Propeller Performance Using Real-coded Genetic Algorithm'. Proceedings of International Propulsion Symposium IPS'10, Okayama, pp. 32-37.

Hess, J.L. & Smith, A.M.O. (1964). 'Calculation of Nonlifting Potential Flow about Arbitrary Three Dimensional Bodies'. Journal of Ship Research, Vol.8, No.2, pp. 22-44.

Kanemaru, T. & Ando, J. (2009). 'A Numerical Analysis of Steady and Unsteady Sheet Cavitation on a Marine propeller Using a Simple Surface Panel Method "SQCM" '. Proceedings of 1st International Synposium on Marine Propulsor, Trondheim, pp. 372-379.

Lan, C.E. (1974). 'A Quasi-Vortex-Lattice Method in Thin Wing Theory'. Journal of Aircraft, Vol.11, No.9, pp. 518-527.

Wang, M.H. (1985). 'Hub Effects in Propeller Design and Analysis'.PhD Thesis, MIT.